Critical Role of Crystalline Anisotropy in the Stability of Cellular Array Structures in Directional Solidification

Przemek Kopczyński, Wouter-Jan Rappel, and Alain Karma
Department of Physics and Center for Interdisciplinary Research on Complex Systems, Northeastern University, Boston, Massachusetts 02115
(Received 10 June 1996)

We calculate numerically the full Floquet-Bloch stability spectrum of cellular array structures in a symmetric model of directional solidification. Our results demonstrate that crystalline anisotropy critically influences the stability of these structures. Without anisotropy, the stability balloon of cells in the plane of wave number and velocity closes near the onset of morphological instability. With a finite, but even small, amount of anisotropy this balloon remains open and a band of stable solutions persists for higher velocities into a deep cell regime. The width of the balloon depends critically on the anisotropy strength. [S0031-9007(96)01426-3]

PACS numbers: 81.10.Aj, 05.70.Ln, 81.30.Fb

Directional solidification has been an important focus of research in the pattern formation and materials science communities for many years [1]. In a generic experiment, a binary liquid mixture contained between two narrowly spaced glass plates is pulled at constant velocity through an externally imposed temperature gradient. The morphology of the solid-liquid interface depends sensitively on the pulling velocity. Below a critical velocity the planar interface is stable, and above this critical velocity it undergoes the well-known Mullins-Sekerka (MS) instability [2] which gives rise to cellular array structures that can exist for a range of spacings.

Close to the onset of instability, cells are typically of small amplitude, while in an intermediate range of higher velocities, they develop a larger amplitude. The latter structures are marked by deep liquid grooves that determine the scale of the final microsegregation profile inside the solidified alloy, and hence its physical properties. Therefore much effort has been devoted to the search for the instabilities which limit the range of possible stable spacings. However, despite more than three decades since the MS analysis, there is still no coherent picture of cell stability in the low velocity regime of directional solidification that has been traditionally studied experimentally. In addition, it is not known how stability is influenced by crystalline anisotropy that is known to play a crucial role in interfacial pattern formation [3].

This lack of understanding is largely due to the technical difficulty of calculating the stability of nonlinear structures in nonlocal models of diffusion controlled growth, and to the fact that spatially extended arrays can be subject to a broad range of instabilities. These can be either oscillatory or nonoscillatory (steady) and can range in wavelength from the cell spacing λ to very long wavelengths. For these reasons, studies to date have been restricted to analyzing specific secondary instabilities [4–10], or to analyzing all possible instabilities but in a high velocity regime where the diffusive growth problem reduces to local equations [11].

A host of instabilities have so far been identified. These include, in a low-velocity regime, the classic long wavelength Eckhaus instability [4,5], which is generically present in one-dimensional pattern forming systems with a finite band of linearly unstable wave numbers, an instability which reduces the cell spacing by 2 (cell halving) [7,8], an oscillatory instability of deep cells with a wavelength equal to the cell spacing λ [9,10], a parity breaking instability with a wavelength equal to λ, which causes cells to grow asymmetrically [7,11], and, in a high-velocity regime [11], short wavelength oscillatory instabilities with a wavelength which is either equal to twice the cell spacing (2λ-O), or irrationally related to λ (I-O). At present, however, it is not known (i) if any of the low-velocity regime instabilities found so far are actually relevant, that is, if they directly bound the band of stable spacings, and (ii) if any of the instabilities found at high velocity pertain to the low velocity regime.

In this Letter, we present the results of the first numerical stability calculations of steady-state cells in directional solidification in which perturbations on all wavelengths of the array are considered (i.e., the full Floquet-Block stability spectrum is calculated). This allows us to identify unambiguously the relevant instabilities and to construct the complete stability balloon for cells in the plane of wave number $q = 2\pi/\lambda$ and velocity V above the onset velocity V_c of the MS instability.

Our first finding is the existence of instabilities with a wavelength equal to twice the cell spacing which always supersede the usual long wavelength Eckhaus instability, except in a negligibly small velocity range close to the onset. One of them is the aforementioned 2λ-O instability, which is also present at high velocity [11] and limits the array stability at large spacing. The other is a new instability with a wavelength also equal to twice λ, but which is steady (2λ-S) and limits the array stability

at small spacing. Physically, this instability gives rise to cell elimination (i.e., a local doubling of the cell spacing) and originates from the nonlocal interaction between cells via the diffusion field.

Our second, and more important, finding is that crystalline anisotropy has a crucial influence on the size of the stability balloon. With zero anisotropy, there are no stable steady states above a maximum velocity which is relatively close to V_c, and therefore the stability balloon closes, while, with some anisotropy above a small critical value, the stability balloon does not close and stable deep cells are present at higher velocity. Moreover, the width of the balloon depends sensitively on the anisotropy strength. Although our findings are for the symmetric model with equal diffusivity D in both phases, we expect the same general picture concerning the role of anisotropy to extend to the one-side model.

We study the equations of directional solidification for a dilute binary alloy in two dimensions

$$\partial_t u = D\nabla^2 u + V\partial_z u\,, \tag{1}$$

$$u_i = 1 - d_0(1 + 15\epsilon\cos 4\theta)\kappa - \xi/l_T\,, \tag{2}$$

$$[k + (1-k)u_i]v_n = -D(\partial_n u|_L - \partial_n u|_S)\,, \tag{3}$$

with a fourfold anisotropy in surface energy. Here $u \equiv (C - C_\infty)/\Delta C_0$ is the dimensionless concentration field, C is the actual concentration, C_∞ is the initial alloy composition, $\Delta C_0 = C_\infty(1/k - 1)$ is the miscibility gap of the planar interface, $d_0 = \Gamma/|m|\Delta C_0$ is the chemical capillary length, Γ is the Gibbs-Thomson coefficient, k is the partition coefficient, m is the liquidus slope, $l_T = |m|\Delta C/G$ is the thermal length where G is the temperature gradient, κ is the interface curvature, ξ is the z coordinate of the interface, v_n is the normal velocity of the interface and V the pulling velocity of the sample, and ϵ is the small parameter which measures the strength of anisotropy in surface energy. All the results presented here are for a value of $k = 0.9$ and a fixed value of $d_0/l_T = 1.14 \times 10^{-3}$. For these parameters, the dimensionless onset velocity $V_c d_0/D = 2.69 \times 10^{-3}$. We examined the velocity range between V_c and $6V_c$, which ranges from small to large amplitude cells as shown in Fig. 1, and varied the anisotropy from 0% to $1\frac{1}{2}$% ($\epsilon \in [0, 0.015]$).

Numerical procedure.—Our numerical stability calculations are based on the now standard boundary integral approach [4–7,10], which makes it possible to recast Eqs. [1–3] into a single integral equation [6,7]. Our procedure consists of three main steps. In the first step, we construct the steady-state interface shapes $\mathbf{r}_q^0(s) = x_q^0(s)\hat{x} + \xi_q^0(s)\hat{z}$ of wave number q, where s_q is the arclength. In the second step, we calculate the stability spectrum by linearly perturbing the steady states with a shift along the normal direction of the general form

$$\mathbf{r}_q = \mathbf{r}_q^0(s) + \mathbf{n}_q^0(s)\delta_{q,Q}(s)\exp[iQ\lambda s/s_q^0 + \omega(Q;q)t]\,,$$

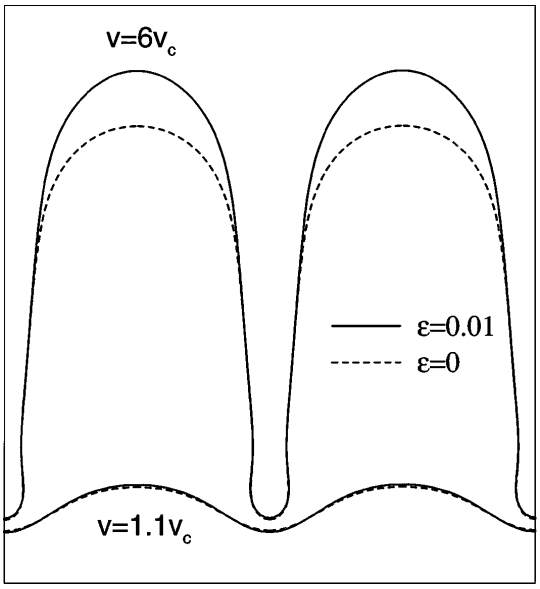

FIG. 1. Calculated steady-state shapes for 0% and 1% anisotropy.

where $\mathbf{n}_q^0$ is the normal unit vector s_q^0 is the total arclength of the cell over one complete period [i.e., $x_q^0(s + s_q^0) = x_q^0(s) + \lambda$], and $Q/q \in [0, 1/2]$ is the Bloch wave vector. The Floquet-Bloch theorem implies that $\delta_{q,Q}(s)$ is a function which has the same periodicity as the underlying steady states: $\delta_{q,Q}(s + s_q^0) = \delta_{q,Q}(s)$. This calculation is equivalent to calculating the stability of a cellular array of infinite spatial extent against perturbations of all possible wavelengths. The complex growth rate of the perturbation $\omega(Q;q)$ is then obtained by solving the eigenvalue problem resulting from the discretized linear integral equation. This second step in the calculation uses the quasistationary approximation which consists in letting $\partial_t u = 0$ in the diffusion equation. It therefore allows us to obtain exactly the neutral stability boundaries of all possible nonoscillatory modes. These boundaries are not affected by this approximation since $\omega(Q,q)$ vanishes identically on them. The positions of the neutral stability boundaries of oscillatory instabilities, however, depend crucially on this approximation. To predict those accurately, we perform in a third step a stability analysis that includes the $\partial_t u$ term in the diffusion equation [12]. Rather than performing a Floquet-Bloch analysis, as in the quasistationary approximation, we have used a previously developed method [10] which determines the stability of cellular arrays in a computational box of length $L = n\lambda$ against perturbations with wavelengths smaller or equal to L. Long wavelength instabilities can be investigated by choosing more cells in the computational box which enables us to construct the Floquet-Block spectrum. In summary, the above three steps allow us to identify the neutral stability boundaries of all possible wavelength

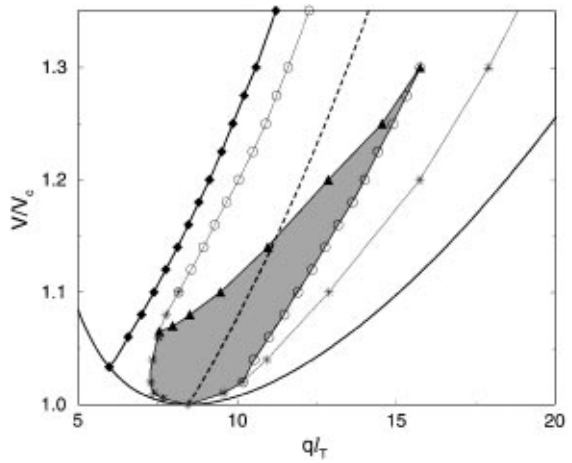

FIG. 2. Stability balloon (shaded area) without anisotropy in the plane of wave number q and velocity V. Shown are the neutral stability boundaries of various modes: Eckhaus (stars), 2λ-S (open circles), and 2λ-O (filled triangles). Also shown are the neutral stability boundary of the planar interface (solid line), the most unstable wave number (dashed line), and $q_{\min}$ (filled diamonds).

perturbations of the array for the full diffusion problem with $\partial_t u \neq 0$. Our results are presented in Figs. 2–5.

Relevant instabilities.—Both with zero (Fig. 2) and finite (Fig. 3) anisotropy, the Eckhaus instability is only relevant very close to the onset. It is first superseded on the large-q side of the stability balloon by the 2λ-S instability. Cells are stable between the left and right neutral stability boundaries of this instability, but only the right boundary bounds the balloon as shown explicitly in Fig. 2. It is then superseded on the small-q side of this balloon by the 2λ-O instability.

Therefore the short wavelength 2λ-S and 2λ-O instabilities are the most relevant ones for cellular structures in the present model since they directly bound almost the entire stability balloon in both Figs. 2 and 3. These instabilities correspond to real (2λ-S) and complex (2λ-O) branches of the stability spectrum $\omega(Q;q)$ which bifurcate at the edge $Q/q = 1/2$ of the first Brillouin zone as shown in Fig. 5.

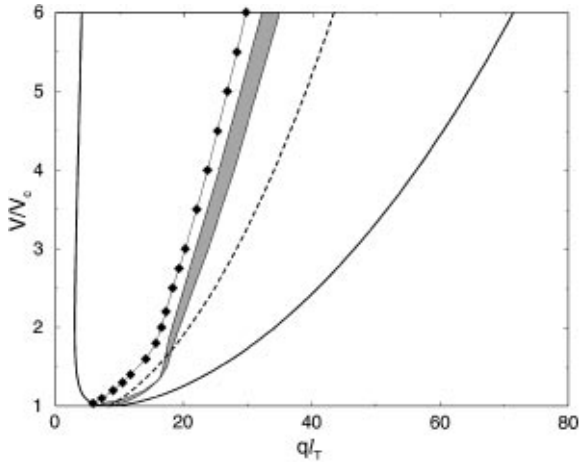

FIG. 3. Stability balloon with 1% anisotropy. The symbols demarking the boundaries of the limiting instabilities are omitted for clarity. The other lines are defined as in Fig. 2.

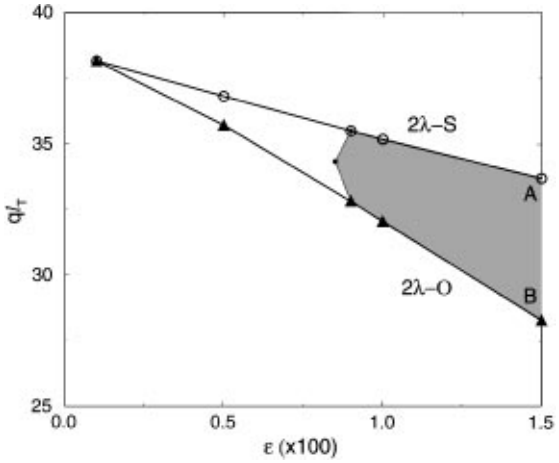

FIG. 4. Stability balloon in the plane of anisotropy and wave number for $V = 6V_c$. The balloon is terminated at small anisotropy by an irrational oscillatory mode I-O with a wavelength longer than 2λ (dashed line).

The stability balloon without anisotropy is qualitatively similar to the one obtained in the high velocity limit by Kassner *et al.* where Eqs. (1)–(3) can be reduced to a local equation [11]. One main difference, however, is the presence here of the 2λ-S instability, which is absent in the high velocity limit where the Eckhaus boundary remains the limiting instability at small spacing. Interestingly, a similar 2λ-S instability, which is possibly related to the present one, has also been found to limit the stability of dendrite arrays at small spacing [13].

Role of anisotropy.—This role can be directly seen by contrasting Figs. 2 and 3, which show the stability balloons for 0% and 1% anisotropy, respectively. Without anisotropy, the balloon closes at a velocity, which

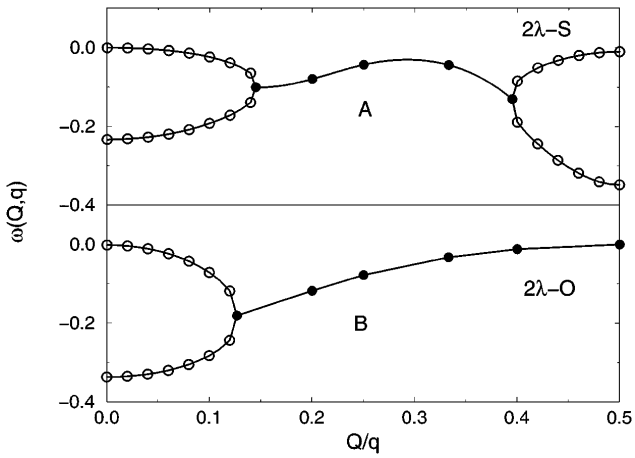

FIG. 5. Floquet-Bloch spectrum for points A and B in Fig. 4. The solid and open circles correspond to complex and real values of $\omega(Q,q)$, respectively.

is only about 30% larger than V_c due to the crossing of the neutral stability boundaries of the dominant short wavelength modes. With anisotropy, the balloon remains open for higher velocities in the deep cell regime. The role of anisotropy is further revealed in Fig. 4, which shows the stability balloon as a function of anisotropy and wave number at a fixed velocity in this regime. The width of the stable band increases dramatically with anisotropy and is almost two times larger for $1\frac{1}{2}\%$ anisotropy than for 1%. Furthermore, the balloon closes at a lower critical anisotropy due to the irrational oscillatory instability (I-O).

Other instabilities.—We have denoted in Fig. 2 by diamonds the boundary ($q_{\min}$) that marks the small-q limit of existence of the main branch of steady-state cells. Crossing of this boundary by increasing V at fixed q leads to the cell halving described by Ramprasad and Brown [8]. Cells, however, are already unstable before this boundary is reached such that it is not directly relevant here. Further from the onset, the small-q limit of the main branch of steady-state cells corresponds to a fold (i.e., limit point) in this branch. This fold coincides with the zero crossing of a real branch of $\omega(Q;q)$ at $Q = 0$ and the onset of a localized tip-splitting mode. Tip splitting has been traditionally interpreted as a limit of stability for cells [14]. Here the boundary of this mode does not bound the stability balloon. This boundary, however, is relatively close and runs parallel to that of the 2λ-O mode up as shown in Fig. 3. This proximity suggests that it may be difficult to distinguish between these two instabilities. This may explain why tip splitting is more commonly observed experimentally, although 2λ- oscillations have also been seen in numerical simulations [15]. Omitted from Fig. 2 is the neutral stability boundary of the parity-breaking instability to tilted cells which lies outside the stability balloon [7]. Finally, the previously found oscillatory instability of deep cells on one wavelength [9,10] is only present for much larger q and also lies outside this balloon.

We conclude with a few remarks concerning the relevance of our results for experiment. Figure 3 shows that the most unstable wave number of the planar interface crosses the band of stable wave numbers. This crossing agrees qualitatively with experimental results to date, which have consistently found that the most unstable wave number is smaller than the experimentally observed cell wave number near the onset [16,17], but larger than the latter far from onset [18]. A more important implication of our results is that *stable* cellular array structures should not be generically observable without anisotropy except very close to the onset. This is qualitatively consistent both with the recent experiments of Akamatsu *et al.* [19], who observed a spatiotemporally chaotic growth morphology when they (effectively) eliminated anisotropy by a judicious choice of grain orientation, and with their numerical simulations of the one-sided model with zero anisotropy which reveal a similar behavior. What remains to be understood is whether the relatively narrow band of spacings present with anisotropy can be accessed dynamically starting from realistic initial conditions. This does not seem obvious since there may exist other attractors for the dynamics even if this stable band is present. Or this band may be too narrow to be selected in which case it would only become an attractor at larger anisotropy where it is much broader. These pattern selection issues are currently being investigated using a phase field approach [20].

This research was supported by DOE Grant No. DE-FG02-92ER45471 and benefited from CRAY time at the National Energy Resources Supercomputer Center.

[1] W. Kurz and R. Trivedi, Acta Metall. **38**, 1 (1990).
[2] W. W. Mullins and R. F. Sekerka, J. Appl. Phys. **34**, 323 (1963).
[3] J. S. Langer, in *Chance and Matter*, Lectures on the Theory of Pattern Formation, Les Houches, Session XLVI, edited by J. Souletie, J. Vannimenus, and R. Stora (North-Holland, Amsterdam, 1987), p. 629–711; D. Kessler, J. Koplik, and H. Levine, Adv. Phys. **37**, 255 (1988).
[4] J. S. Langer, Acta Metall. **25**, 1121 (1977).
[5] K. Brattkus and C. Misbah, Phys. Rev. Lett. **64**, 1935 (1990).
[6] D. A. Kessler and H. Levine, Phys. Rev. A **39**, 3041 (1989).
[7] H. Levine, W.-J. Rappel, and H. Riecke, Phys. Rev. A **43**, 1122 (1991).
[8] N. Ramprasad and R. A. Brown, Phys. Rev. B **38**, 583 (1988).
[9] A. Karma and P. Pelcé, Phys. Rev. A **41**, 6741 (1990).
[10] D. A. Kessler and H. Levine, Phys. Rev. A **41**, 3197 (1990); W.-J. Rappel and E. A. Brener, J. Phys. I (France) **2**, 1779 (1992).
[11] K. Kassner, C. Misbah, H. Mueller-Krumbhaar, and A. Valence, Phys. Rev. E **49**, 5477 (1994).
[12] This step relaxes the quasistationary approximation used to calculate the boundary of oscillatory modes in an earlier unpublished study.
[13] J. A. Warren and J. S. Langer, Phys. Rev. A **42**, 3518 (1990); Phys. Rev. E **47**, 2702 (1993).
[14] S. Lu and J. D. Hunt, J. Cryst. Growth **123**, 17 (1992); J. D. Hunt and S. Lu, Mater. Sci. Eng. A **173**, 79 (1993).
[15] B. Grossmann, K. R. Elder, M. Grant, and J. M. Kosterlitz, Phys. Rev. Lett. **71**, 3323 (1993).
[16] D. Liu, L. M. Williams, and H. Z. Cummins, Phys. Rev. E **50**, R4286 (1994).
[17] S. de Cheveigne, C. Guthmann, and M. M. Lebrun, J. Cryst. Growth **73**, 242 (1985).
[18] M. A. Eshelman and R. Trivedi, Acta Metall. **35**, 2443 (1987).
[19] S. Akamatsu, G. Faivre, and T. Ihle, Phys. Rev. E **51**, 4751 (1995).
[20] A. Karma and W.-J. Rappel, Phys. Rev. E **53**, 3017 (1996).